



# The anti-erosion potential of taproots and fibrous roots in alluvial loess of north China: a pot experiment

Zijian Kang<sup>1</sup> · Guochong Lou<sup>1</sup> · Yuanyuan Guo<sup>2</sup> · Peng Xu<sup>1</sup>

Received: 9 August 2023 / Accepted: 22 October 2023 / Published online: 7 November 2023  
© The Author(s), under exclusive licence to Springer-Verlag GmbH Germany, part of Springer Nature 2023

## Abstract

**Purpose** This study aims to investigate the anti-erosion potential of taproots and fibrous roots with different diameters in alluvial loess under the concentrated flow.

**Materials and methods** A pot experiment was conducted in the greenhouse. Alluvial loess widely distributed in north China was used for plant growing. Two herbs, alfalfa (*Medicago sativa*) with taproots and tall festuca (*Festuca arundinacea*) with fibrous roots, were selected for single and mixed planting. Root configuration and soil detachment capacity (Dc) at different depths were measured, then the anti-erosion potential of taproots and fibrous roots with different diameters was analyzed.

**Results and discussion** Fibrous roots exhibited greater root length density (RLD) and fine root (0–1 mm) ratio at all depths, while taproots had larger mean diameter and root volume density (RVD). The Dc was reduced by 25.3–56.6% in the presence of roots compared to soil without roots, and the Dc of single fibrous roots treatment was significantly lower than that of single taproots and mixed roots. Whether in soil containing taproots or fibrous roots, Dc was only significantly negatively correlated with the density of very fine roots (<0.5 mm). In fibrous roots, the direct path coefficient of very fine roots to Dc was significantly higher than that of roots at other diameter classes, while in taproots, the direct path coefficient of coarse roots (> 2 mm) to Dc was highest.

**Conclusions** Variations in root diameter (<0.5, 0.5–1, 1–2, > 2 mm) distribution and root density are important factors contributing to differences in Dc at different depths. In alluvial loess with low clay and high silt content, the high density of very fine roots (<0.5 mm) in fibrous roots is critical for demonstrating greater anti-erosion potential. The presence of more medium roots (1–2 mm) and coarse roots (> 2 mm) is the main reason for decreasing in the anti-erosion potential of taproots.

**Keywords** Alluvial loess · Pot experiment · Taproots · Fibrous roots · Root configuration · Soil detachment capacity

## 1 Introduction

Loess soil is one of the most erosion-prone soils in the world, so engineering constructions in loess regions not only have to ensure their structural stability but also face constant erosion control challenges (Wen and Zhen 2020; Feng and Li 2021). With the continuous development of China's transportation network, the conflict between highway construction

and environmental protection is becoming more and more intense. The exposed slope left by highway construction in the loess region has caused serious soil erosion and environmental imbalance, which has gradually become a major obstacle to the stable operation of highways in the later stages (Tao et al. 2023; Huang et al. 2018). Therefore, it is particularly vital to restore the natural environment, control soil losses, and avoid soil erosion disasters by soil bioengineering in loess regions (Giupponi et al. 2019; Bischetti et al. 2021).

Water erosion is the most widespread and damaging type of soil erosion in the world, with the main forms being rain-drop splash erosion, sheet erosion, gully erosion, and scouring erosion (Prats et al. 2019; Luo et al. 2018). Exposed loess slopes are more vulnerable to water erosion than ordinary soil slopes, which exacerbates soil and water loss until serious soil erosion disasters such as collapse, landslide, and debris flow occur (Chen and Zhang 2022; Tao et al.

Responsible editor: Claudio Bini

✉ Guochong Lou  
louguochong\_stdu@163.com

<sup>1</sup> School of Civil Engineering, Shijiazhuang Tiedao University, Shijiazhuang, Hebei 050043, China

<sup>2</sup> School of Architecture & Art, Shijiazhuang Tiedao University, Shijiazhuang, Hebei 050043, China

2023). Plantation protection measures are widely used in bare slope restoration projects by increasing slope vegetation cover, reducing external environmental erosivity, improving soil erosion resistance, and then delaying slope soil erosion (Zou et al. 2022; Yang et al. 2023). Herbaceous plants have rapid ecological regulation ability and extensive adaptability, which is not only considered an ecological answer to solving soil erosion problems but also the important and primary object of bare slope restoration (Reubens et al. 2007; Wang et al. 2022a).

Water erosion of soil is mainly caused by raindrop erosion and surface runoff erosion. Vegetation has a significant effect in reducing these types of erosion. Beeson and Doyle found that the amount of soil erosion in the unvegetated riparian zone was 5 times greater than in the vegetated riparian zone (Beeson and Doyle 1995). The improvement of soil erosion resistance by vegetation can be divided into two aspects: the above-ground part and the underground root system (Li and Pan 2018). In the process of water erosion on slopes, the vegetation canopy is usually the first line of defense, reducing erosion by intercepting rainfall and resisting the impact of rainwater (Liu et al. 2021a). Research on erosion resistance in different types of grasslands shows that the contribution of plant canopies to runoff reduction is as high as 48.8% (Li et al. 2022). The stem of plants and the litter layer formed on the soil surface can also significantly reduce soil water erosion. In the typical grassland of the Loess Plateau, plant stems and the litter layer reduced the soil detachment capacity ( $D_c$ ) by 30.3% and 59% respectively (Wang et al. 2014; Liu et al. 2020).

Research by Gyssels shows that the above-ground portion of vegetation is more effective in controlling soil splash and rill erosion, but is limited to the initial stage of slope erosion (Gyssels 2005). Conversely, the growth of underground plant roots plays a vital role in enhancing soil structure, physical and chemical properties, and microbial distribution, particularly in mitigating flow erosion in the later stages of slope erosion (Stokes et al. 2014). The physical binding of roots and soil can greatly improve the anti-scourability of soil, and roots growth can also effectively promote soil particle aggregation by improving soil organic matter content and microorganisms, thereby improving soil structure and slowing soil disintegration rate (Wang et al. 2020, 2018). Previous studies have shown that plant roots account for more than 50% of the total  $D_c$  reduction caused by subsurface soil properties, highlighting the need to consider the effects of roots in soil anti-erosion studies (Wang and Zhang 2017; Karimi et al. 2022).

The erosion-reducing effect of plant roots depends not only on the number of roots in the soil (such as root length, surface area, volume, etc.), but also on specific root characteristics (such as root type, diameter, tensile strength,

etc.) (Vannoppen et al. 2015; Baets et al. 2007; Liu et al. 2022). A large number of studies have quantified the role of plant roots in reducing erosion. For concentrated flow erosion, root density (RD), root diameter (D), and root length density (RLD) are the most commonly used root characteristics to estimate the erosion reduction potential of plant species (Vannoppen et al. 2016; Baets et al. 2009). At the same time, a mathematical model between soil detachment rate (SDR), root length density (RLD), and root mass density (RD) has been proposed to predict the ability of plant roots to reduce soil erosion (Vannoppen et al. 2017). Under the same root density, the fibrous root system often has a greater ability to reduce erosion than taproots. Finer and denser fibrous roots can better improve soil cohesion by virtue of higher root tensile strength and more root-soil contact (Zhang et al. 2014; Mao et al. 2012). Wang and Zhang also found that the  $D_c$  of taproot grassland was 3.2 times higher than that of fibrous root grassland (Wang and Zhang 2017). Root diameter is an important index of root morphology. The main roots and higher lateral roots of herbaceous plants have larger root diameters, but this does not mean that they have higher erosion resistance potential. By contrast, the improvement of soil anti-scourability was positively correlated with the number of fine roots, and the length density of roots with < 2 mm diameter was the main factor in reducing soil scouring (Li et al. 1992; Hao et al. 2020). At the same time, several studies found that coarse roots had a poor performance in improving soil erosion resistance, and there was a positive correlation between root diameter and  $D_c$  (Stokes et al. 2009; Reubens et al. 2007; Burylo et al. 2012), which may mean that plants characterized by a high proportion of fine roots are the most suitable for reducing soil detachment.

Currently, most studies focus on the effects of soil physical and chemical properties on soil erosion resistance after root action (Guo et al. 2018; Wu et al. 2016). Considering the specificity of alluvial loess, there are few studies on the direct influence of different herbaceous root configurations on soil consolidation and erosion resistance. To solve this problem, two herbaceous plants (alfalfa and tall fescuca) which are widely used in soil bioengineering (Bischetti et al. 2014, 2021; Giupponi et al. 2019), representing taproots and fibrous roots respectively, were selected for a pot experiment to reduce the impact on the heterogeneity of soil properties and climatic parameters. Then the varying root configuration along depth and root anti-erosion potential was investigated in alluvial loess. The purpose of our study is to answer the following questions: (1) What is the spatial distribution of roots in soil? (2) What is the effect of the roots of the two herbaceous plants on  $D_c$ ? (3) What are the differences in the effects of different root types and diameter classes on the anti-erosion ability of alluvial loess?

## 2 Materials and methods

### 2.1 Experimental setup

The soil for the pot experiment was collected from the slope topsoil (5–30 cm) of the Taihang Mountains Expressway, Zhangjiakou Sect. (115.699°E, 40.840°N), as shown in Fig. 1c. The soil texture is silt loam composed of  $72.62 \pm 0.82\%$  silt (0.002–0.05 mm),  $18.11 \pm 0.52\%$  sand (0.05–2 mm), and  $9.27 \pm 0.28\%$  clay (<0.002 mm). The soil organic matter content is  $16.27 \text{ g kg}^{-1}$ . After removing stones and roots, the soil was passed through a 2 mm sieve and dried in an oven (110 °C, 72 h) for the next experiment. The plants were grown in a greenhouse at Shijiazhuang Tiedao University, as shown in Fig. 1(d). In the greenhouse, the temperature is maintained at 25–32 °C during the day and 15–20 °C at night. The light is 16 h per day, the darkness is 8 h, and the air humidity is 75%.

PVC pipes (11 cm in diameter and 25 cm in height) were used as containers for plant growth. These PVC pipes were cut in half lengthwise and then held together with two rigid hoops. At the bottom of the container, a layer of sponge wrapped one end of the PVC pipe for water permeability, and a plastic plate was placed at the bottom of each container to hold water and indirectly irrigate the soil through the bottom sponge. Alfalfa (taproots) and tall fescue (fibrous roots) are selected as plant research objects because these two types of plants have the characteristics of fast growth and strong stress resistance, which are widely used in ecological restoration (Ai et al. 2020). Four different depth ranges (0–5, 5–10, 10–15, and 15–20 cm) were set to study the changes in root distribution and soil anti-erosion ability with depth. There were four treatments, including single alfalfa

(SA), single tall fescue (ST), mixed two types of plants (M), and plant-free control treatment (CK). Each treatment was repeated 4 times, with a total of 16 pots.

Before sowing, the dried soil was filled into PVC pipes in four times, each filling 670 g. After each filling, the soil in pipes was gently shaken and compacted to control the height of each filling to 5 cm, and the dry bulk density of the soil was  $1.4 \text{ g cm}^{-3}$  (He et al. 2022). After four fillings, a further 1 cm of soil was added as the sowing layer. The total weight of seeds in each treatment was 0.4 g, with the M treatment containing two kinds of seeds, each weighing 0.2 g. One week after sowing, the emergence of seedlings was observed and the number of plants in each pot was controlled at 15 plants, then plants were grown continuously for 150 days. To prevent soil structure from being damaged by supplementary water, water was added to the bottom plate for irrigating indirectly in the first month, and each pot of plant was watered with 100 ml daily. In the future growth time, each pot of plant was watered 2–3 times a week for 300 ml. Among them, 100 ml of water is directly irrigated through topsoil and 200 ml is indirectly irrigated through bottom plates.

### 2.2 Laboratory experiment

After the growth period, the above-ground part of the plants and a 1 cm layer of topsoil were carefully removed from containers. The rigid hoops surrounding the PVC pipes were opened, and the PVC pipes were subsequently removed to obtain the complete soil columns. Using a ring knife (inner diameter 9 cm, height 4 cm), a soil sample was taken every 5 cm along the depth direction. Concentrated flow experiments were first carried out on these soil samples and then the root parameters in the soil were determined.

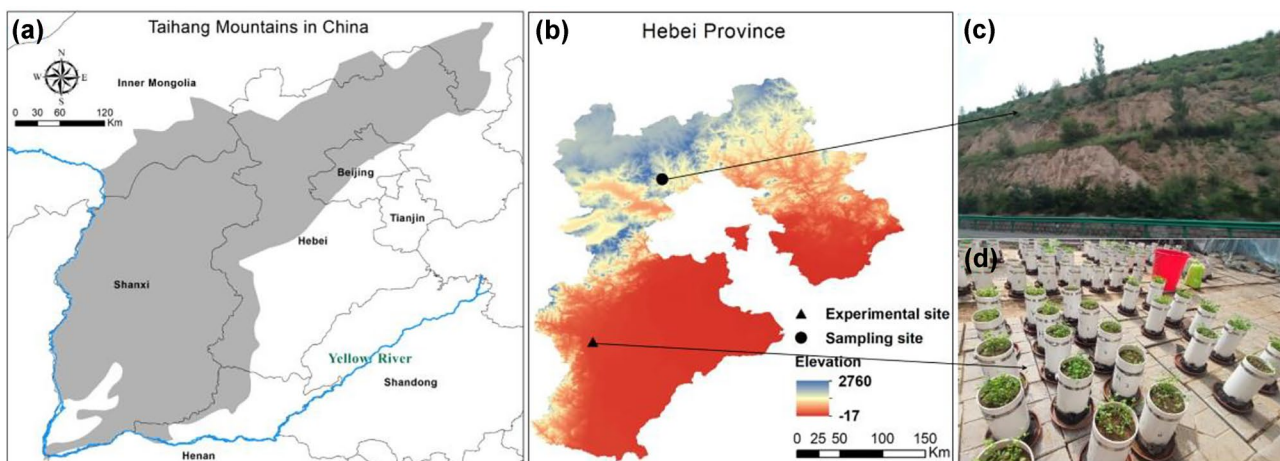


**Fig. 1** The area of Taihang Mountains in China (a, b) and the location of soil sampling (c) and greenhouse experiment sites (d)

### 2.2.1 Concentrated flow erosion experiment

Concentrated flow erosion was tested in a hydraulic flume with 3 m long, 0.2 m wide, and 0.2 m deep (Fig. 2). There is a steady flow tank on the top of the flume and a circular sample room (0.09 m diameter, 0.04 m deep) at a distance of 0.2 m from the bottom of the flume. The inclination angle of the flume is 15°. The water pump pumps the water from the circular water tank into the steady flow tank at a flow rate of 4.8 L min<sup>-1</sup>, allowing the water to flow out evenly from one side of the steady flow tank.

After sampling, two permeable stones were placed at the bottom and the top of the soil sample respectively, and then they were put into a water tank where the water level does not exceed the permeable stone at the sample bottom. The water was poured continuously on the top permeable stone until those samples to be tested are fully saturated, and then samples were removed from the water tank and placed for 8 h to remove gravity water. Before the scouring test, the soil sample was placed in the sample room, and the gap between the soil sample and the flume was filled with glass glue to reduce the marginal effect. During the scouring test, plastic buckets were used to collect water scouring soil samples. The scouring number is 6 times and the single scouring time is 40 s. After the scouring test, all collected water samples were left to stand for 5 h, then the supernatant was poured out, and the remaining water was filtered with filter paper. The filtered sample was dried in an oven at 105 °C for 24 h, and the dry weight of the

scoured soil was calculated. Soil detachment capacity ( $D_c$ ) is used to reflect the anti-scouring performance of the soil, and the calculation formula is:

$$D_c = \frac{M_c}{At} \quad (1)$$

where  $M_c$  (g) is the drying weight of sediment;  $A$  (cm<sup>2</sup>) is the cross-sectional area of soil core;  $t$  (s) is the duration of erosion.

### 2.2.2 Root parameter

After scouring, the remaining soil sample containing roots was collected and put on a 0.25 mm sieve to separate the roots from the soil by washing, then the roots in scouring water were also separated by sieve. These roots were carefully collected from the sieve with tweezers, and then cleaned again with a detergent solution to remove the fine soil particles as much as possible. After cleaning, the root system was placed into a transparent petri dish (add clean water) to take pictures with a camera. The mean diameter ( $D$ ), root length, root surface area, and root volume of the root system were analyzed by Rhizo Vision Explorer software (Rose et al. 2019). Root parameters, root length density (RLD), root surface density (RSAD), and root volume density (RVD) were calculated using Eqs. (2)–(4).

$$RLD = \frac{RL}{V} \quad (2)$$

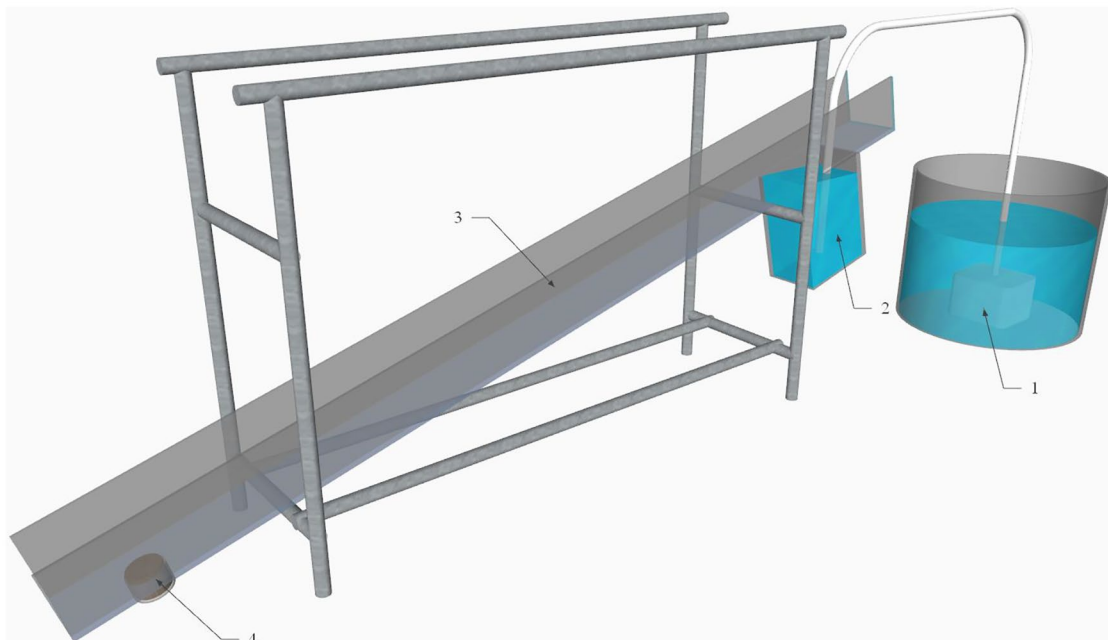


**Fig. 2** The experimental flume used to measure the soil detachment capacity. 1, water tank and bump; 2, Steady flow tank; 3, Scoured flume; 4, Sample room

$$RSAD = \frac{RSA}{V} \quad (3)$$

$$RVD = \frac{RV}{V} \quad (4)$$

where RL (cm) is the total root length in the sample; RSA (cm<sup>2</sup>) is the total root surface area in the sample; RV (cm<sup>3</sup>) is the total root volume in the sample; and V (cm<sup>3</sup>) is the sampler volume.

### 2.3 Statistical analysis

Least-Significant Difference (LSD) tests were performed ( $P < 0.05$ ) to analyze the difference of root density (RLD, RSAD, RVD, and D) in different treatments and soil depths. Pearson correlation analysis was applied to assess the relationships between root parameters and Dc. Regression analysis was performed to establish the correlations between Dc and root parameters (RLD, RSAD, RVD, and D). Path analysis was used to determine the importance of root parameters at different diameter classes on Dc. All analyses were performed using SPSS 26.0 software and Origin 2021 software.

## 3 Results

### 3.1 Plants root configuration and vertical distribution

In Table 1, the RLD of ST treatment was significantly higher than that of SA and M at almost every depth ( $P < 0.05$ , Except for 5–10 cm of M), but the RVD and D of ST were lower than that of SA and M, especially in the depth of 0–10 cm.

With increasing soil depth, the RLD of single planting treatments (ST, SA) first decreased and then increased, and the greater root length density appeared in the surface layer (0–5 cm) and bottom layer (15–20 cm). The RLD of M treatment initially increased and then decreased with depth, and the RLD at 0–10 cm depth was higher than that at 10–20 cm depth. RSAD, RVD, and D of the three root treatments decreased with soil depth, and these root parameters in surface soil (0–5 cm) were significantly higher than in deeper soil (10–20 cm). In 0–10 cm depth, the order of D is SA > M > ST, but in 10–20 cm depth, the order of D is M > SA > ST.

The distribution of root length, surface area, and volume at different diameter classes in soil containing roots is presented in Fig. 3. The length proportion of very fine roots (< 0.5 mm) was highest in the three treatments. In ST treatment, the length proportion of very fine roots is 70.71–87.59%, while in SA and M, the length proportion of very fine roots is 53.4–78.19%. With increasing soil depth, the length ratio of very fine roots gradually increased in SA and ST, while decreased first and then increased in M. In each treatment, the length ratio of fine roots (0.5–1 mm) is 12.31–37.90%. The total proportion of medium roots (1–2 mm) and coarse roots (> 2 mm) was less than 10% and gradually decreased with soil depth in all treatments. In the SA and M treatments, the coarse roots only appeared at 0–10 cm depth, and ST had no coarse roots in all depths. Compared to the root length proportion, the surface area and volume proportion of very fine roots are lower, while the situation of fine roots, medium roots, and coarse roots was just the opposite. In the 0–5 cm depth of SA, 53.4% of very fine root length brought 29.34% of surface area and 11.76% of volume, but 2.88% of coarse root length brought 11.31% of surface area and 29.58% of volume.

**Table 1** Total root parameters at different depths of each treatment

| Treatment | Soil depth (cm) | Total root parameters      |  |   |                |
|-----------|-----------------|----------------------------|--|---|----------------|
|           |                 | RLD (mm cm <sup>-3</sup> ) | RSAD (mm <sup>2</sup> cm <sup>-3</sup> ) | RVD (mm <sup>3</sup> cm <sup>-3</sup> ) | D (mm)         |
| ST        | 0–5             | 104.88 ± 8.44abA           | 148.90 ± 21.61aA                         | 21.59 ± 4.55aB                          | 0.47 ± 0.04aB  |
|           | 5–10            | 89.78 ± 8.52bA             | 119.70 ± 14.74abAB                       | 15.94 ± 2.57abB                         | 0.45 ± 0.02aB  |
|           | 10–15           | 101.77 ± 15.20abA          | 115.15 ± 23.57abA                        | 10.93 ± 2.91bA                          | 0.34 ± 0.02bB  |
|           | 15–20           | 112.22 ± 12.02aA           | 107.25 ± 15.21bA                         | 9.49 ± 1.97bA                           | 0.30 ± 0.02bB  |
| SA        | 0–5             | 70.75 ± 5.42abB            | 137.56 ± 4.14aA                          | 30.59 ± 6.38aAB                         | 0.67 ± 0.08aA  |
|           | 5–10            | 61.73 ± 7.85bB             | 110.17 ± 16.41abB                        | 21.49 ± 5.10aAB                         | 0.61 ± 0.04aA  |
|           | 10–15           | 66.22 ± 5.34bB             | 94.48 ± 5.81bA                           | 12.78 ± 2.94bA                          | 0.47 ± 0.07bA  |
|           | 15–20           | 79.13 ± 6.55aB             | 92.23 ± 1.39bA                           | 9.70 ± 1.32bA                           | 0.37 ± 0.04bA  |
| M         | 0–5             | 80.73 ± 8.63abB            | 159.23 ± 17.64aA                         | 35.75 ± 6.06aA                          | 0.63 ± 0.07aA  |
|           | 5–10            | 87.18 ± 7.34aA             | 145.42 ± 13.61aA                         | 26.67 ± 4.87aA                          | 0.54 ± 0.05aA  |
|           | 10–15           | 70.31 ± 6.35bB             | 107.23 ± 9.76bA                          | 15.62 ± 2.74bA                          | 0.48 ± 0.03abA |
|           | 15–20           | 76.32 ± 8.94abB            | 99.83 ± 18.87bA                          | 12.00 ± 1.89bA                          | 0.40 ± 0.04bA  |

Different lowercase letters indicates significant differences at  $P < 0.05$  between different depths. Different capital letter indicates significant differences at  $P < 0.05$  between different treatment

RLD Root length density, RSAD Root surface area density, RVD Root volume density, D Average diameter

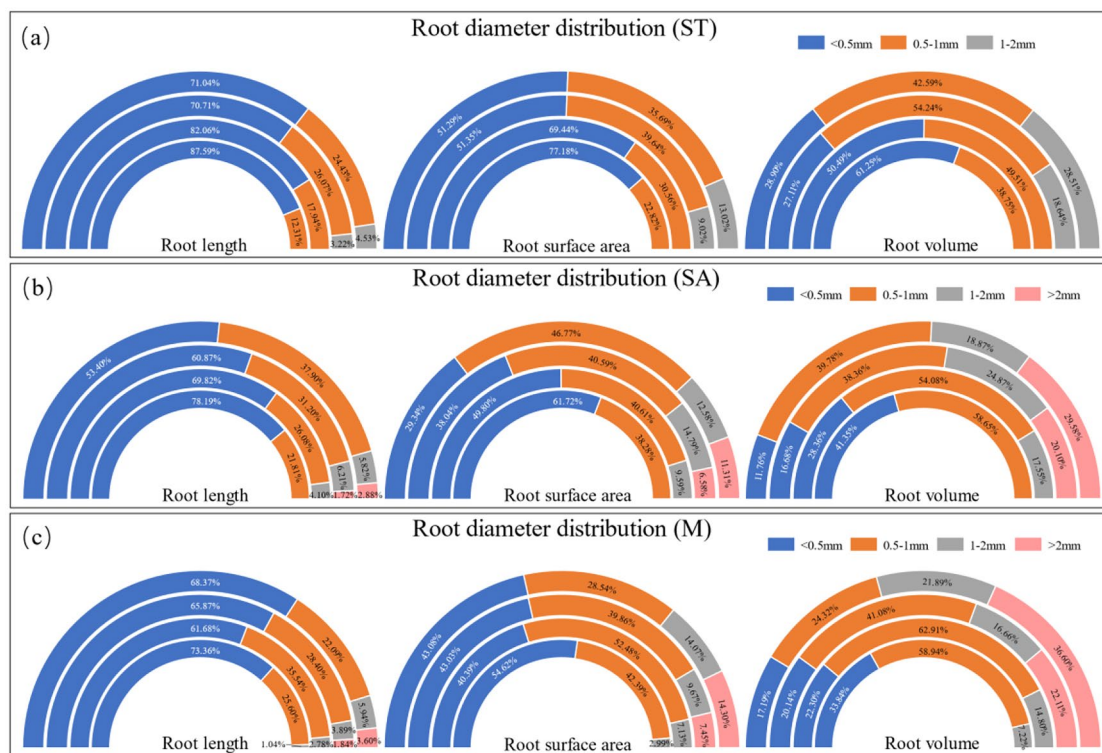


**Fig. 3** Root length, surface area, and volume distribution of different diameter classes. The circular plot shows the root diameter distribution within soil depths of 0–5 cm, 5–10 cm, 10–15 cm, and 15–20 cm from the outside to the inside, respectively

### 3.2 Soil detachment capacity under concentrated flow

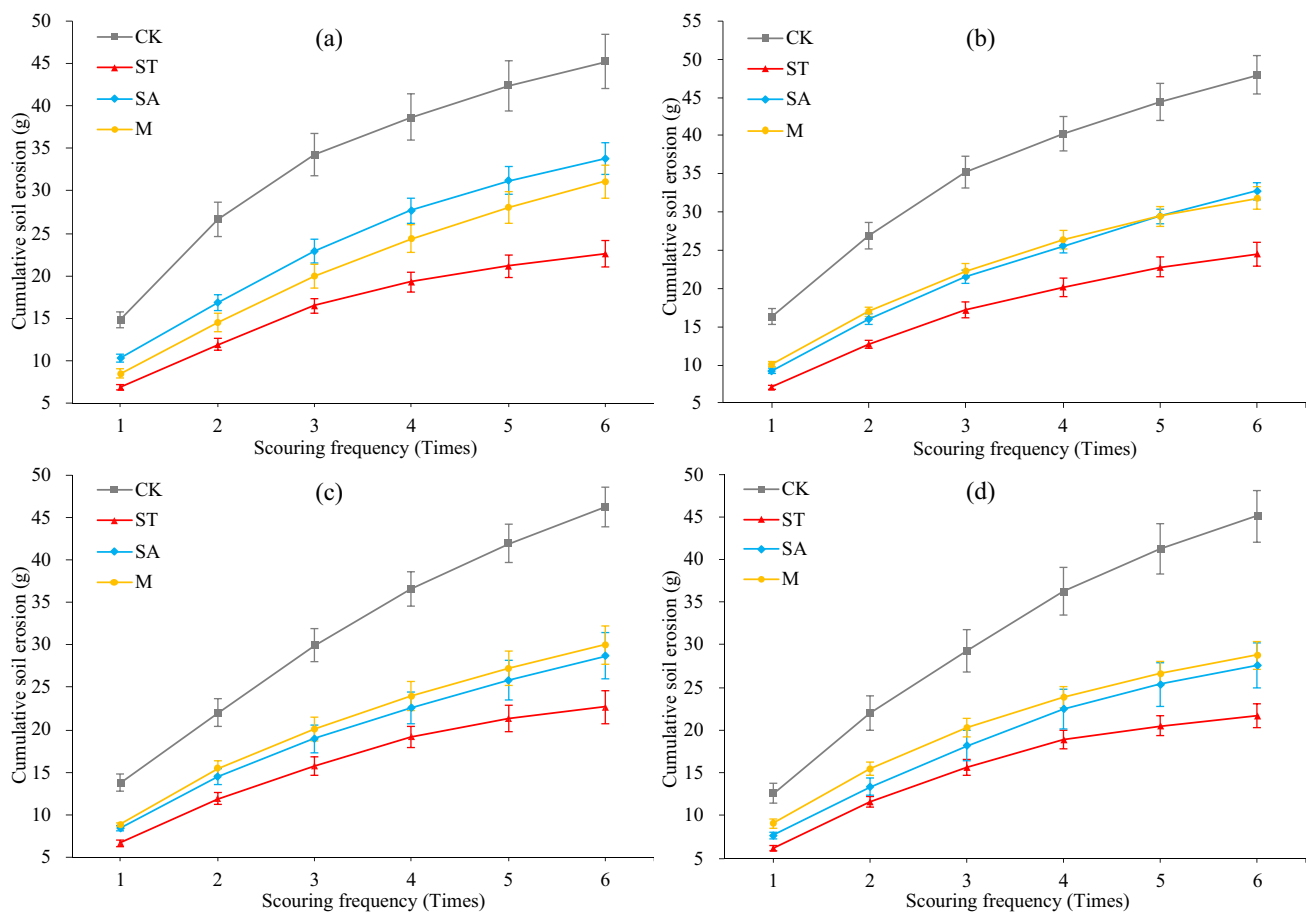
The cumulative soil erosion at different depths is shown in Fig. 4. The cumulative erosion of soil without roots was significantly higher than that of soil containing roots ( $P < 0.05$ ), in which the total scouring sediment of plain soil at each depth was in the range of 45.07–47.94 g, while that of root-containing soil was 21.66–33.79 g. Soil erosion of ST treatment was significantly lower than that of SA and M treatments ( $P < 0.05$ ). Compared to CK treatment, the cumulative erosion reduction rate of ST was 48.79–51.94%, while that of SA and M was 25.28–38.78% and 31.27–36.12%, respectively. At the same time, the cumulative erosion reduction ratio of root-containing soil increased with soil depth. In the range of 0–5 cm depth, the cumulative erosion curve of M treatment is between SA and ST, while in the range of 10–20 cm, the cumulative erosion curve of M is higher than that of SA and ST.

Figure 5 shows the single erosion quantity of each treatment at different depths. The first erosion quantity of each treatment approximately accounted for 30% of the cumulative soil erosion, among which the first erosion quantity of CK at different depths was in the range of 12.61–16.33 g, while those of ST, SA, and M were 6.17–7.09 g, 7.66–10.31 g,

and 8.43–10.07 g, respectively. With the increase of scouring times, single soil erosion of each treatment gradually decreases. The single erosion curves in 0–10 cm depth for each treatment were generally higher than those in 10–20 cm depth. In addition, the difference between the single erosion curves of different soil layers in ST and M was small, while in the CK and SA treatment, the curves between different depth ranges varied more.

### 3.3 Soil detachment capacity and total root parameters

Changes in initial soil detachment capacity ( $D_{c1}$ ) and total soil detachment capacity ( $D_{cT}$ ) with depth are shown in Fig. 6. Planting significantly ( $P < 0.05$ ) reduced  $D_{c1}$  and  $D_{cT}$ . At different depths, the range of  $D_{c1}$  in plain soil is 49.55–64.17  $\text{g m}^2 \text{s}^{-1}$ , and that of  $D_{cT}$  is 29.52–31.40  $\text{g m}^2 \text{s}^{-1}$ . The range of  $D_{c1}$  in soil containing roots was 24.26–40.59  $\text{g m}^2 \text{s}^{-1}$ , and that of  $D_{cT}$  was 14.19–22.13  $\text{g m}^2 \text{s}^{-1}$ . The  $D_{c1}$  and  $D_{cT}$  of ST were significantly lower than those of SA and M at all depths ( $P < 0.05$ ). At 0–5 cm depth, SA treatment had higher  $D_{c1}$  and  $D_{cT}$  than M, while at 10–20 cm depth, M had higher  $D_{c1}$  and  $D_{cT}$ . With increasing soil depth, the  $D_c$  ( $D_{c1}$ ,  $D_{cT}$ ) of ST, M, and CK first increased and then decreased, while that of SA decreased gradually.



**Fig. 4** The cumulative soil erosion at each depth of different treatments. Figures (a), (b), (c), and (d) show the cumulative erosion changes in 0–5 cm, 5–10 cm, 10–15 cm, and 15–20 cm depths, respectively

The fitting relationships between soil detachment capacity ( $Dc_1$ ,  $Dc_t$ ) and total root parameters (RLD, RSAD, RVD, D) are shown in Fig. 7. Whether in the taproots or fibrous roots, there was a linear decrease relationship between RLD and  $Dc$  in Fig. 5(a) and (e). Among them, the RLD of ST (fibrous root) had a good fitting relationship with  $Dc_1$  and  $Dc_t$ , and the goodness of fit was 0.7128 and 0.8623 respectively. In Fig. 7(b), (c), (f), and (g), the RSAD and RVD of fibrous roots have a poor fitting relationship with  $Dc_1$  and  $Dc_t$ , but both RSAD and RVD of taproots have a good linear growth relationship with  $Dc_1$  and  $Dc_t$ , and these goodness of fit were 0.7031, 0.6064, 0.8186, and 0.7706. The mean diameter (D) increases linearly with  $Dc_1$  but has a poor fitting relationship with  $Dc_t$  in fibrous roots. In addition, the mean diameter showed a good linear growth relationship with  $Dc_1$  and  $Dc_t$  in taproots.

### 3.4 Effects of taproots and fibrous roots in different diameters on soil detachment capacity

The correlation analysis between root parameters at different diameter classes and soil detachment capacity ( $Dc_1$ ,  $Dc_t$ ) is shown in Fig. 8. The results showed that no matter in the fibrous root or taproots, densities of fine roots (0.5–1 mm), medium roots (1–2 mm), and coarse roots (> 2 mm) were positively correlated with each other, but very fine root (< 0.5 mm) density was negatively correlated with them. The very fine root density (RLD<sub><0.5</sub>, RSAD<sub><0.5</sub>, and RVD<sub><0.5</sub>) was negatively correlated with  $Dc_1$  and  $Dc_t$ , and the correlation of fibrous roots was stronger than taproots. In fibrous roots, the density of fine and medium roots was positively correlated with  $Dc_1$  and had no significant correlation with  $Dc_t$ , while

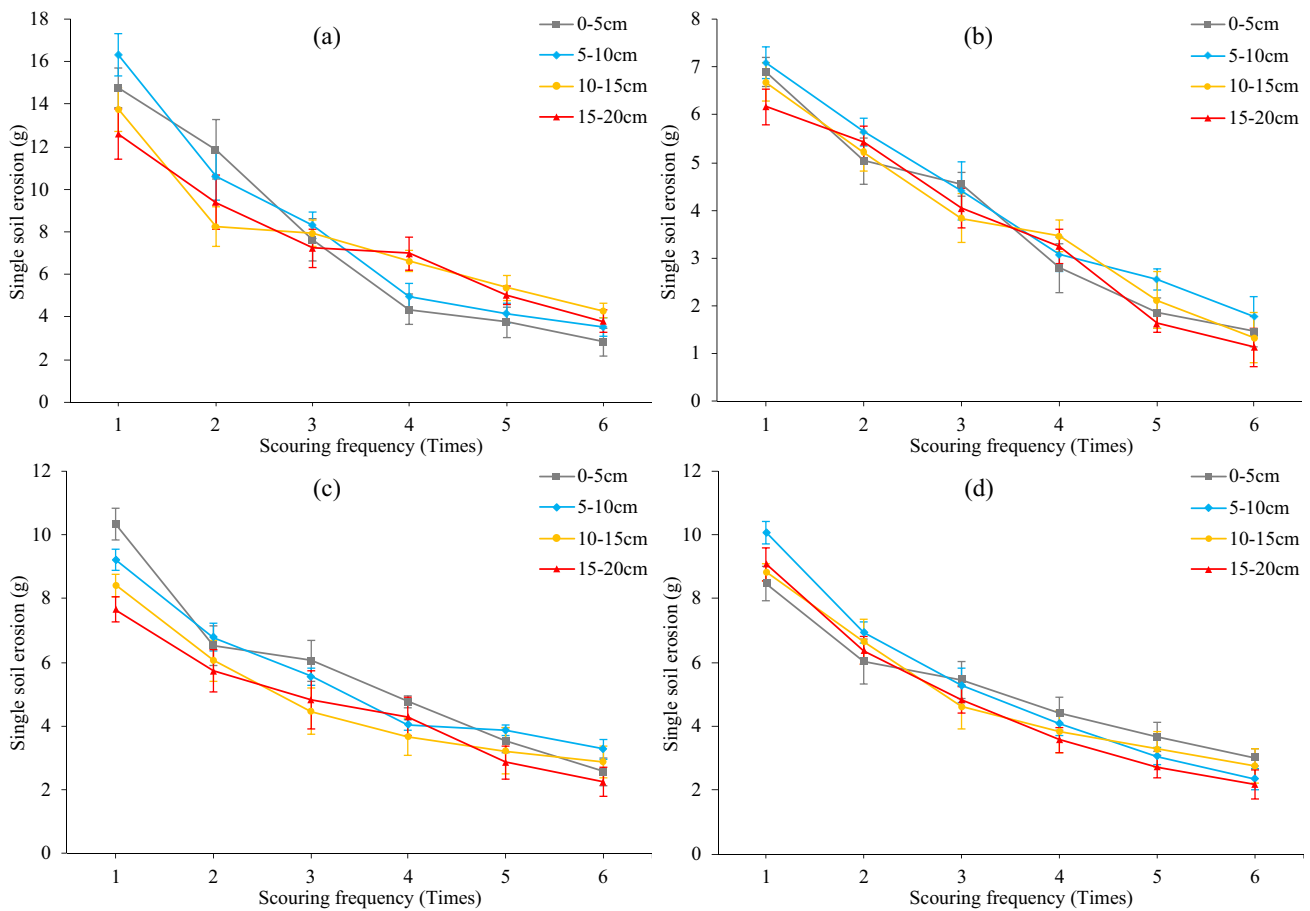


**Fig. 5** The single soil erosion at different depths. Figures (a), (b), (c), and (d) show the changes in single erosion amount of CK, ST, SA, and M treatments, respectively

in taproots, densities of fine roots, medium roots, and coarse roots were positively correlated with  $Dc_1$  and  $Dc_t$ . Due to the correlation analysis can only determine the

relationship between root parameters and  $Dc$ , it is necessary to use path analysis to study the main factors affecting soil erosion.

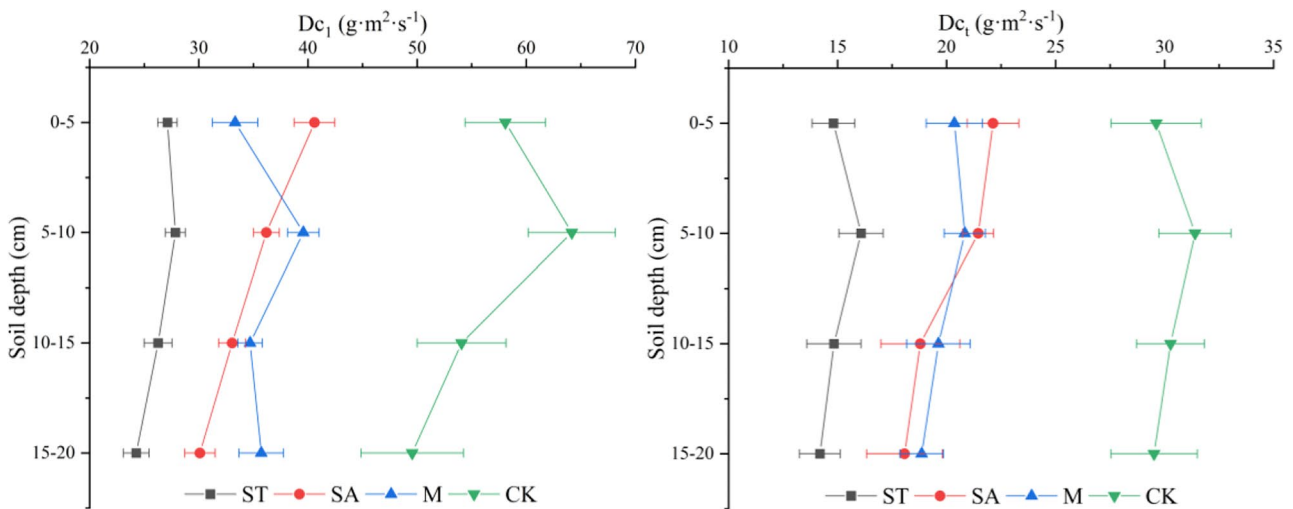


**Fig. 6** Soil detachment capacity ( $Dc_1$ ,  $Dc_t$ ) of each treatment at different depths



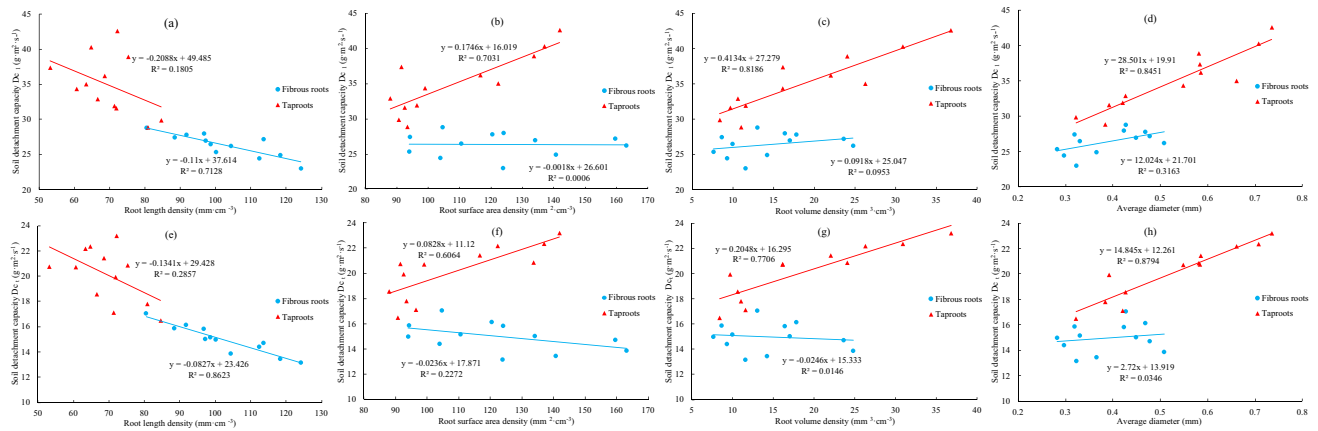


**Fig. 7** The relationship between total root parameters (RLD, RSAD, RVD, and D) and soil detachment capacity ( $D_{c1}$ ,  $D_{c2}$ ), where (a), (b), (c), and (d) are root parameters of fibrous roots, and (e), (f), (g), and (h) are root parameters of taproots

In our study, there was an extreme correlation among RLD, RSAD, and RVD at the same diameter class, so path analyses of RLD, RSAD, and RVD in different diameters were carried out separately. First of all, the normality test of  $D_{c1}$  and  $D_{c2}$  was conducted. For the small sample of  $n = 12$ , the Shapiro–Wilk Test method was used. The result shows that  $D_{c1}$  and  $D_{c2}$  obey normal distribution and can be analyzed by regression. These results of normality tests can be referred to in the supplementary Fig. 1(a)–(d). The direct

and indirect effects of root parameters in different diameters on soil detachment capacity ( $D_{c1}$ ,  $D_{c2}$ ) are shown in Fig. 9, Tables 2 and 3. Some path analysis results of RSAD and RVD can be referred to in the Supplementary Tables 1–4.

In fibrous roots,  $RLD_{<0.5}$  is the leading factor to explain the changes of  $D_{c1}$  and  $D_{c2}$ , and the direct path coefficient is -0.989 and -1.132. In addition, the indirect path coefficients of  $RLD_{<0.5}$  passing through  $RLD_{0.5-1}$  and  $RLD_{1-2}$  to  $D_{c1}$  and  $D_{c2}$  are also larger (Table 2). In Fig. 9a and b, RVD and RSAD



**Fig. 8** Correlation results between the soil detachment capacity ( $D_{c1}$ ,  $D_{c2}$ ) and root parameters in different diameters. Among them, relevant results of fibrous roots is at the lower left of this picture, while taproots is at the top right of this picture

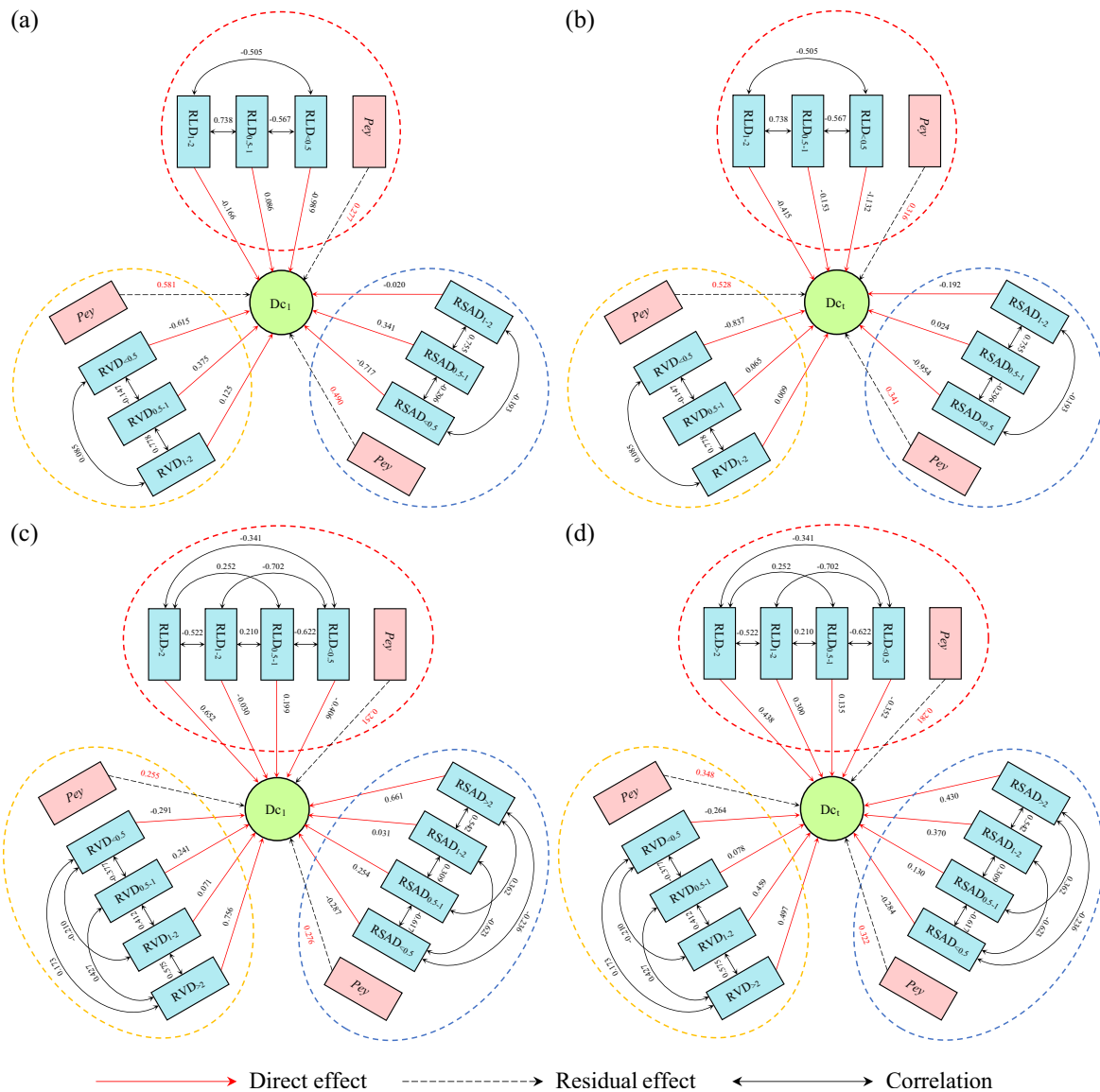


**Fig. 9** Path analysis diagram of influencing factors of soil detachment capacity ( $Dc_1$ ,  $Dc_I$ )

of fine roots (0.5–1 mm) have a higher -direct path coefficient for  $Dc_1$  than RLD, and RLD of medium roots (1–2 mm) have a higher direct path coefficient for  $Dc_I$  than RVD and RSAD. The residual path coefficients of RLD in different

diameters to  $Dc_1$  and  $Dc_I$  were 0.277 and 0.316 respectively, while those of RSAD and RVD were 0.490, 0.341, and 0.581, 0.528. This shows that different diameter classes of RLD can explain more changes in  $Dc$ .

**Table 2** The path analysis of RLD at different classes and  $Dc$  in fibrous roots

| Independent variable | Direct path coefficient |        | Indirect path coefficient |                |                |                |                |                |
|----------------------|-------------------------|--------|---------------------------|----------------|----------------|----------------|----------------|----------------|
|                      | $Dc_1$                  | $Dc_I$ | $X_1$ - $Dc_1$            | $X_2$ - $Dc_1$ | $X_3$ - $Dc_1$ | $X_1$ - $Dc_I$ | $X_2$ - $Dc_I$ | $X_3$ - $Dc_I$ |
| $X_1$                | -1.132                  | -0.989 | -                         | -0.642         | -0.572         | -              | -0.561         | -0.499         |
| $X_2$                | 0.153                   | 0.086  | -0.087                    | -              | 0.113          | -0.049         | -              | 0.063          |
| $X_3$                | 0.415                   | 0.166  | -0.210                    | 0.306          | -              | -0.084         | 0.123          | -              |

$Dc_1$  total soil detachment capacity,  $Dc_I$  initial soil detachment capacity,  $X_1$  root length density of <0.5 mm (RLD<sub><0.5</sub>),  $X_2$  root length density of 0.5-1 mm (RLD<sub>0.5-1</sub>),  $X_3$  root length density of 1-2 mm (RLD<sub>1-2</sub>)

**Table 3** The path analysis of RLD at different classes and Dc in taproots

| Independent variable | Direct path coefficient |        | Indirect path coefficient |            |            |            |            |            |            |            |
|----------------------|-------------------------|--------|---------------------------|------------|------------|------------|------------|------------|------------|------------|
|                      | $Dc_t$                  | $Dc_l$ | $X_1-Dc_t$                | $X_2-Dc_t$ | $X_3-Dc_t$ | $X_4-Dc_t$ | $X_1-Dc_l$ | $X_2-Dc_l$ | $X_3-Dc_l$ | $X_4-Dc_l$ |
| $X_1$                | -0.352                  | -0.406 | -                         | -0.219     | -0.247     | -0.120     | -          | -0.253     | -0.285     | -0.138     |
| $X_2$                | 0.135                   | 0.199  | -0.084                    | -          | 0.028      | 0.034      | -0.124     | -          | 0.042      | 0.050      |
| $X_3$                | 0.300                   | -0.030 | -0.211                    | 0.063      | -          | 0.157      | -0.021     | 0.006      | -          | 0.016      |
| $X_4$                | 0.438                   | -0.652 | -0.149                    | 0.110      | 0.229      | -          | -0.222     | 0.164      | 0.340      | -          |

$Dc_t$  total soil detachment capacity,  $Dc_l$  initial soil detachment capacity,  $X_2$  root length density of 0.5–1 mm (RLD<sub>0.5–1</sub>),  $X_3$  root length density of 1–2 mm (RLD<sub>1–2</sub>),  $X_4$  root length density of > 2 mm (RLD<sub>>2</sub>)

In taproots, the density of coarse roots (> 2 mm) was the main factor to explain changes in Dc (Table 3). The direct path coefficient of very fine roots density to  $Dc_l$  is the second after coarse roots density in RLD, but for  $Dc_t$ , medium roots have a higher direct path coefficient than very fine roots in RSAD and RVD (Fig. 9c and d). The residual path coefficient of taproots configuration parameters for  $Dc_l$  is lower than that for  $Dc_t$ , and residual path coefficients of RLD, RSAD, and RVD on Dc ( $Dc_l$ ,  $Dc_t$ ) are similar in the taproots system, while in the fibrous root system, the residual path coefficient of RLD on Dc is obviously smaller than RVD and RSAD, especially for  $Dc_l$ .

## 4 Discussion

In the soil, the plant roots of developed from main roots or superior lateral roots tend to be thicker, which play the role of skeleton and support (Stokes et al. 2009). The fine roots of plants are usually lateral and fibrous roots that cross each other and extend in all directions, and fine roots have the basic physiological function of being able to absorb and transport more nutrients and water from the soil, which is closely related to the physical and chemical properties of the soil (Yang et al. 2014). Therefore, the configuration and distribution of roots can reflect the ability of plants to utilize soil resources to some extent (Guerrero-Campo et al. 2006). Based on these characteristics, plant roots of different species and diameters play various roles and importance in the soil ecosystem.

The root morphological differences among different species are mainly reflected in the topsoil because more than 70% of the root parameters are distributed in the upper soil with 0–20 cm (Ye et al. 2017), so we investigated the vertical distribution characteristics of root systems in the range of surface 20 cm depth for taproots and fibrous roots. In the wild environment, the roots of herbaceous plants are mainly composed of roots with a diameter lower than 2 mm (Chimento and Amaducci 2015). He et al. also found that the fibrous root length with < 0.5 mm diameter accounted for the vast majority, and the root content of > 1 mm diameter class was smaller (He et al. 2022). This is in agreement with our research

results. Among the three planting treatments in this study, the length proportion of very fine root (< 0.5 mm) was the largest, in the range of 53.4% to 87.59%, followed by fine root (0.5–1 mm), accounting for 12.31–37.9%, and the root length density with > 1 mm diameter only accounted for 3.22–9.54%. In our study, taproots and fibrous roots exhibited significant differences when root density (RLD, RSAD, RVD) was used to quantify root distribution. Fibrous roots had higher RLD, while the average diameter of taproots was significantly ( $P < 0.05$ ) higher than that of fibrous roots. Although the RLD of taproots was smaller, a higher root diameter brought more RSAD and RVD (Wang et al. 2023). Under the same growth conditions, these differences in root distribution may be affected by their own physiological characteristics, nutrient acquisition, and competition (Deljouei et al. 2022).

The differentiation of plant roots is often adapted to their growth needs to survive in adversity and disturbance (Klimešová and Herben 2021; Tao et al. 2021; Pang et al. 2022). For example, differences in root types will affect the extension of roots in the soil. Taproots tend to have stronger soil penetration than fibrous roots, and thick RD is generally considered to be the primary advantage of taproots over fibrous roots in penetrating hard soil (He et al. 2022). To ensure that the soil density is roughly the same, our soil is compacted before sowing. Taproots with strong penetrating ability can reach the deep soil earlier, and root networks can be established quickly in the deeper soil. Therefore, in the early stage of root underground competition, the growth space of fibrous roots in soil may be reduced (Cramer et al. 2012). We found that the distribution of very fine roots in M treatment was close to that of ST in the depth of 0–10 cm, while in the depth of 10–20 cm, the root distribution of M treatment was similar to that of SA. This could mean that alfalfa roots (taproots), as a dominant competitive species, restrict the growth and development of tall fescue (fibrous root) to deeper soil. Under the premise of controlling access to water and nutrients, dominant species usually adopt more active foraging strategies, which increase their root length, root surface area, or root volume, and increase the contact area between roots and soil to obtain more soil nutrient resources (Li et al. 2014; Hodge 2006). While the growth of fibrous roots in deep soil is limited, the

difference in root distribution caused by taproots intraspecific competition may also appear. Previous studies have shown that herbaceous plants tend to have lower root length, surface area, and diameter under high-density conditions (Sun et al. 2018). In our study, the plant density of the dominant competitor (alfalfa) in M was half of that in SA treatment. In the depth range of 10–20 cm, the M treatment which should have more fine roots showed a higher average diameter than SA.

Due to the boundary effect caused by the culture container, the vertical distribution of roots may be different from the real situation in the field (Tian et al. 2017). Previous studies have shown that plant roots under field conditions are often concentrated in the topsoil, and the total root density decreased with depth (Ye et al. 2017; Zhong et al. 2018; Yang et al. 2022). In this study, a large number of roots grow in the gap between culture containers (PVC pipes) and soil, which means that the lateral growth of roots is limited. Under the guidance of foraging strategies, there is no doubt that the roots will more grow into the soil where water and nutrients may appear (Wang et al. 2022b). Because the water supply in our experiment comes from trays at the bottom of culture containers, this may cause the root system to grow more and extend to the deep soil layer, and this increase in foraging size may be the main reason for the high total root density in the lower soil (10–20 cm).

soil bioengineering technique is an effective way to reduce soil erosion, in which root reinforcement is considered to be the main source of soil erosion protection (Lou et al. 2022). Compared to shrubs and trees, herbaceous plants and their roots are often the first to protect the soil and lay the foundation for other plants growing because of their rapid growth and adaptability, so herbs are widely used in the restoration and protection of bare soil (Gao et al. 2022; Zanchi et al. 2022; Gomes et al. 2020). Rill erodibility ( $K_r$ ) can better reflect the change of soil erosion resistance, in which the effect of herbaceous plants is more significant. Compared with the control field, the average  $K_r$  of herbaceous vegetation restoration soil decreased by 72% to 96% (Zhang et al. 2019). In addition, when considering the underground part of the plant alone, the reduction rate of herbaceous plant root exfoliation to soil was more than 40% (Jiang et al. 2020). In our study, the soil detachment capacity ( $D_c$ ) of root-containing treatment decreased by 25.3–56.6% compared to treatment without roots, which further demonstrated the anti-erosion potential of herbaceous plant roots.

The temporal and spatial differences in rooted soil detachment capacity are partly caused by changes in soil physicochemical properties under the influence of plant roots (Li et al. 2015; Jiang et al. 2020). Roots can connect soil particles by interlacing, inserting, binding, and squeezing, and then improving the soil structure and strengthening the soil (Reubens et al. 2007; Li et al. 2017). In addition, root exudates and litter can continuously transport organic matter

to the soil (Shahzad et al. 2015). These organic matter and its decomposition products can act as colloids between soil aggregates, thereby improving aggregate stability and soil cohesion, and improving soil erosion resistance (Wang et al. 2014; Baets et al. 2008; Zhang et al. 2019). Due to the different functional positioning of fine and coarse roots in the soil, their abilities to control soil erosion are different (Stokes et al. 2009; Geng and Jin 2022). In soil, coarse roots are an important root structure and the main water transport channel, therefore the extension direction of coarse roots during growth is mostly downward (Baets et al. 2007). However, fine roots need to absorb more nutrients from the soil and diverge in various directions during growth, making it easier to form anchoring relationships in shallow soil and protect the surface soil (Yang et al. 2014; Reubens et al. 2007). Finer and denser fibrous roots can also reduce the large pore space used for water movement, while the high porosity brought by coarse roots promotes water movement toward deeper soil, which may accelerate soil erosion (Lu et al. 2020). At present, fine roots have been proven to be a key factor in changing soil erosion resistance characteristics, the influence of roots in controlling soil detachment capacity largely depends on the number of fine roots and their distribution in soil (Hao et al. 2020).

Previous studies also proved that the soil erosion resistance of plant roots became stronger with the increase of RLD (Fu et al. 2022). In our study, the minimum detachment capacity of root-containing soil appeared in depth with higher RLD. Compared with RSAD and RVD, RLD in planting treatment could better reflect the change of  $D_c$ . Whether the initial soil detachment capacity ( $D_{c1}$ ) or the total soil detachment capacity ( $D_c$ ), the residual path coefficient after the influence of each diameter class RLD was relatively small. Compared to fibrous roots, the residual path coefficient of taproots density to  $D_c$  is smaller, and the density of medium root and coarse root has higher relative importance. However, the effect of these thicker roots and fine roots on  $D_c$  seems to be different. Due to the interspersed growth of roots in the soil, thicker roots will destroy the original structure of the soil to some extent. Many studies have found that the ability of roots to reduce soil detachment decreased with the increase in root diameter (Baets et al. 2007; Parhizkar et al. 2021). Burylo et al. found that soil detachment rate (SDR) was negatively correlated with the percentage of fine roots (<0.5 mm) (Burylo et al. 2012). This is consistent with our results.

Compared with taproots, fibrous roots formed a complex fine root network through their strong root tillering ability and showed stronger soil and water conservation ability (Zhao et al. 2023). We also found that the  $D_c$  of single fibrous roots treatment was significantly lower than that of single taproots and mixed roots at each depth, which was undoubtedly caused by the difference in root type and configuration. The main root even aggravates soil erosion because the soil around the

exposed thick root is washed away more under the action of turbulence and vortex flow erosion (Baets et al. 2007). In our experiment process, we did find that there were more exposed roots in the soil samples with taproots. Most of these roots are coarse roots (> 2 mm) and the surrounding soil is looser. In addition, the rapid soil detachment caused by exposed roots may aggravate the marginal effect between soil samples and flume, thus increasing the soil detachment rate under the influence of local turbulence (Wang et al. 2019).

Altogether, the erosion intensity of soil decreased with the increase of soil cohesion. Previous researches have found that fibrous roots are usually more effective than taproots in controlling soil loss, especially in non-clay (Vannoppen et al. 2017, 2015). The growth and development of fibrous roots have been proven to be more effective in increasing soil cohesion, even a small amount of fibrous roots would increase soil cohesion to a certain extent (Zhong et al. 2016). Therefore, fibrous roots in low cohesion soils tend to have better erosion resistance performance. Loess is easily eroded due to its texture and structure. Although loess has high cohesion and stability at low water content, its cohesion will dissipate rapidly with the increase of water content, and it is unrealistic to maintain low water content under the action of water erosion (Liu et al. 2021b). Therefore, in the alluvial loess with low clay content, the anti-erosion effect of fibrous roots may be magnified. As an important difference index of root configuration, root diameter may explain the difference in anti-erosion potential of straight and whisker roots to some extent. In the alluvial loess of our study, the erosion resistance potential of very fine roots (<0.5 mm) is significantly higher than that of roots in other diameters because only the density of very fine roots is negatively correlated with Dc, but these results do not mean that the coarse root has completely lost its anti-erosion potential. Coarser roots are more effective in soil with low sand content (Vannoppen et al. 2017). At the same time, affected by the morphological characteristics of taproots, the soil protection effect through coarse root anchorage in large-scale soil may be higher than in the local shallow soil (Stokes et al. 2009). But it is undeniable that in alluvial loess, fibrous roots show more strength in the process of controlling concentrated flow erosion by virtue of high-density fine roots. Meanwhile, with the growth and development of plant roots, the anti-erosion contribution of coarser taproots was gradually covered by high-density fibrous roots and even showed a negative contribution.

## 5 Conclusions

Pot experimental observations demonstrated that in the taproot and fibrous root, the length of very fine roots (<0.5 mm) accounted for the largest proportion (53.4–87.59%), especially in the fibrous root system of deeper soil (10–20 cm).

The length of > 1 mm roots accounted for less than 10% and more occurs in taproot systems of shallow soil. Both taproots and fibrous roots can effectively reduce the concentrated flow erosion of alluvial loess, with a reduced rate of 25.3% and 56.6%. Among them, fibrous roots have a greater potential for reducing soil detachment. The distribution of finer roots is an important factor affecting the anti-erosion potential. Only very fine roots (<0.5 mm) density was significantly negatively correlated with soil detachment capacity (Dc), and coarser roots are not even conducive to resistance to soil erosion. Whether taproots or fibrous roots, RLD in different diameters could explain the majority of the changes in Dc, while RSAD and RVD of fibrous roots had a relatively low explanation extent. According to our novel findings, in alluvial loess with low clay and high silt content, the erosion resistance potential of very fine roots in fibrous roots is much greater than that of other diameter roots, which is similar to the results in sandy soil with low cohesion. The density of coarse roots (> 2 mm) in taproots also has a greater effect on Dc, but this effect is more disadvantageous. In locally shallow soil, the anti-erosion potential of coarser roots is masked by finer roots. Therefore, in alluvial loess areas, the soil bioengineering dominated by fibrous root plants has more advantages in controlling soil erosion.

**Supplementary Information** The online version contains supplementary material available at <https://doi.org/10.1007/s11368-023-03678-6>.

**Acknowledgements** We are grateful to Kuoyu Zhao for supplying the experimental soil (Hebei Traffic Planning Design Institute) and Rende Wang (Institute of Geographical Sciences Hebei Academy of Sciences) for the testing of soil physical and chemical properties. Zijian Kang acknowledges support from the Key R & D projects in Hebei Province (19274207D).

**Data availability** The data that support the findings of this study are available from the corresponding author, [Yuanyuan Guo], upon reasonable request.

## Declarations

**Conflict of interest** We declare no conflict of interest.

## References

- Ai YJ, Li FP, Gu HH, Chi XJ, Yuan XT, Han DY (2020) Combined effects of green manure returning and addition of sewage sludge compost on plant growth and microorganism communities in gold tailings. *Environ Sci Pollut R* 27(25):31686–31698. <https://doi.org/10.1007/s11356-020-09118-z>
- Baets S, De J, Poesen AK, Galindo P (2007) Impact of root architecture on the erosion-reducing potential of roots during concentrated flow. *Earth Surf Proc Land* 32(9):1323–1345. <https://doi.org/10.1002/esp.1470>
- Baets SD, Poesen J, Reubens B, Muys B, De Baerdemaeker J, Meersmans J (2009) Methodological framework to select plant species for controlling rill and gully erosion: application to a

- Mediterranean ecosystem. *Earth Surf Proc Land* 34(10):1374–1392. <https://doi.org/10.1002/esp.1826>
- Baets SD, Torri D, Poesen J, Salvador MP, Meersmans J (2008) Modelling increased soil cohesion due to roots with EUROSEM. *Earth Surf Proc Land* 33(13):1948–1963. <https://doi.org/10.1002/esp.1647>
- Beeson CE, Doyle PF (1995) Comparison of bank erosion at vegetated and non-vegetated channel bends I. *J Am Water Resour* as 31(6):983–990. <https://doi.org/10.1111/j.1752-1688.1995.tb03414.x>
- Bischetti GB, Di Fi Dio M, Florineth F (2014) On the origin of soil bioengineering. *Landsc Res* 39(5):583–595. <https://doi.org/10.1080/01426397.2012.730139>
- Bischetti GB, Giovanni DC, Mickovski SB, Peter RH, Massimiliano S, Rosemarie S (2021) Design and temporal issues in Soil Bioengineering structures for the stabilisation of shallow soil movements. *Ecol Eng* 169:106309. <https://doi.org/10.1016/J.ECOLENG.2021.106309>
- Burylo M, Rey F, Mathys N, Dutoit T (2012) Plant root traits affecting the resistance of soils to concentrated flow erosion. *Earth Surf Proc Land* 37(14):1463–1470. <https://doi.org/10.1002/esp.3248>
- Chen B, Zhang X (2022) Effects of slope vegetation patterns on erosion sediment yield and hydraulic parameters in slope-gully system. *Ecol Indic* 145:109723. <https://doi.org/10.1016/J.ECOLIND.2022.109723>
- Chimento C, Amaducci S (2015) Characterization of fine root system and potential contribution to soil organic carbon of six perennial bioenergy crops. *Biomass Bioenerg* 83:116–122. <https://doi.org/10.1016/j.biombioe.2015.09.008>
- Cramer MD, Wakeling JL, Bond WJ (2012) Belowground competitive suppression of seedling growth by grass in an African savanna. *Plant Ecol* 213(10):1655–1666. <https://doi.org/10.1007/s11258-012-0120-7>
- Deljouei A, Cislighi A, Abdi E, Borz SA, Majnounian B, Hales TC (2022) Implications of hornbeam and beech root systems on slope stability: from field and laboratory measurements to modelling methods. *Plant Soil* 483(1–2):547–572. <https://doi.org/10.1007/S11104-022-05764-Z>
- Feng W, Li Y (2021) Measuring the ecological safety effects of land use transitions promoted by land consolidation projects: the case of Yan'an City on the Loess Plateau of China. *Land* 10(8):783. <https://doi.org/10.3390/LAND10080783>
- Fu Yu, Wang D, Sun W, Guo M (2022) Impacts of grass planting density and components on overland flow hydraulics and soil loss. *Land Degrad Dev* 34(1):234–249. <https://doi.org/10.1002/LDR.4456>
- Gao R, Ai N, Liu G, Liu C, Qiang F, Zhang X, Xiang T, Zang K (2022) The coupling relationship between herb communities and soil in a coal mine reclamation area after different years of restoration. *Forests* 13(9):1481. <https://doi.org/10.3390/F13091481>
- Geng P, Jin G (2022) Fine root morphology and chemical responses to N addition depend on root function and soil depth in a Korean pine plantation in Northeast China. *For Ecol Manag* 520:120407. <https://doi.org/10.1016/J.FORECO.2022.120407>
- Giupponi L, Boronovo G, Giorgi A, Bischetti GB (2019) How to renew soil bioengineering for slope stabilization: some proposals. *Landsc Ecol Eng* 15(1):37–50. <https://doi.org/10.1007/s11355-018-0359-9>
- Gomes L, Miranda HS, Soares Filho B, Rodrigues L, Oliveira U, Bustamante MMC (2020) Responses of plant biomass in the Brazilian Savanna to frequent fires. *Front for Glob Change* 3:50771. <https://doi.org/10.3389/FFGC.2020.507710>
- Guerrero-Campo J, Palacio SARA, Perez-Rontome C, Montserrat-Marti G (2006) Effect of root system morphology on root-sprouting and shoot-rooting abilities in 123 plant species from eroded lands in north-east Spain. *Ann Bot* 98(2):439–447. <https://doi.org/10.1093/aob/mcl122>
- Guo M, Wang W, Kang H, Yang Bo (2018) Changes in soil properties and erodibility of gully heads induced by vegetation restoration on the Loess Plateau, China. *J Arid Land* 10(5):712–725. <https://doi.org/10.1007/s40333-018-0121-z>
- Gyssels G (2005) Impact of plant roots on the resistance of soils to erosion by water: a review. *Prog Phys Geog* 29(2):189–217. <https://doi.org/10.1191/0309133305pp443ra>
- Hao H, Di H, Jiao X, Wang J, Guo Z, Shi Z (2020) Fine roots benefit soil physical properties key to mitigate soil detachment capacity following the restoration of eroded land. *Plant Soil* 446(1):487–501. <https://doi.org/10.1007/s11104-019-04353-x>
- He Y, Zhangli Wu, Zhao T, Yang H, Ali W, Chen J (2022) Different plant species exhibit contrasting root traits and penetration to variation in soil bulk density of clayey red soil. *Agron J* 114(1):867–877. <https://doi.org/10.1002/AGJ2.20972>
- Hodge A (2006) Plastic plants and patchy soils. *J Exp Bot* 57(2):401–411. <https://doi.org/10.1093/JXB/ER1280>
- Huang X, Lili W, Qian Lu (2018) Vulnerability assessment of soil and water loss in loess plateau and its impact on farmers' soil and water conservation adaptive behavior. *Sustainability-Basel* 10(12):4773–4773. <https://doi.org/10.3390/su10124773>
- Jiang F, He K, Huang M, Zhang L, Lin G, Zhan Z, Li H, Lin J, Ge H, Huang Y (2020) Impacts of near soil surface factors on soil detachment process in benggang alluvial fans. *J Hydrol* 590:125274. <https://doi.org/10.1016/j.jhydrol.2020.125274>
- Karimi Z, Abdi E, Deljouei A, Cislighi A, Shirvany A, Schwarz M, Hales TC (2022) Vegetation-induced soil stabilization in coastal area: an example from a natural mangrove forest. *CATENA* 216:106410. <https://doi.org/10.1016/J.CATENA.2022.106410>
- Klimešová J, Herben T (2021) The hidden half of the fine root differentiation in herbs: nonacquisitive belowground organs determine fine-root traits. *Oikos* 2023(1). <https://doi.org/10.1111/OIK.08794>
- Li C, Pan C (2018) The relative importance of different grass components in controlling runoff and erosion on a hillslope under simulated rainfall. *J Hydrol* 558:90–103. <https://doi.org/10.1016/j.jhydrol.2018.01.007>
- Li H, Ma Q, Li H, Zhang F, Rengel Z, Shen J (2014) Root morphological responses to localized nutrient supply differ among crop species with contrasting root traits. *Plant Soil* 376(1/2):151–163. <https://doi.org/10.1007/s11104-013-1965-9>
- Li P, Wang B, Yang Y, Liu G (2022) Effects of vegetation near-soil-surface factors on runoff and sediment reduction in typical grasslands on the Loess Plateau, China. *J Arid Land* 14(03):325–340. <https://doi.org/10.1007/S40333-022-0007-Y>
- Li Q, Liu G-B, Zhang Z, Tuo D-F, Bai R-r, Qiao F-F (2017) Relative contribution of root physical enlacing and biochemical exudates to soil erosion resistance in the Loess soil. *CATENA* 153:61–65. <https://doi.org/10.1016/j.catena.2017.01.037>
- Li Y, Xu XQ, Zhu XM (1992) Preliminary study on mechanism of plant roots to increase soil anti-scourability on the Loess Plateau. *Sci China Chem* 22(3):254–259. <https://doi.org/10.1360/zb1992-22-3-254>
- Li Z-W, Zhang G-H, Geng R, Wang H (2015) Spatial heterogeneity of soil detachment capacity by overland flow at a hillslope with ephemeral gullies on the Loess Plateau. *Geomorphology* 248:264–272. <https://doi.org/10.1016/j.geomorph.2015.07.036>
- Liu J-X, Li P-P, Liu G-B, Flanagan DC (2020) Quantifying the effects of plant litter in the topsoil on the soil detachment process by overland flow in typical grasslands of the Loess Plateau, China. *Hydrol Process* 34(9):2076–2087. <https://doi.org/10.1002/hyp.13713>
- Liu X, Dengxing F, Guodong J, Xinxiao Yu (2021a) Quantitative simulation of the particle size distribution of eroded sediment on grass slopes with intact plants and root slopes with the aboveground parts removed. *Soil Sci Soc Am J* 85(2):396–411. <https://doi.org/10.1002/SAJ2.20199>
- Liu Y-B, Xia-song Hu, Dong-mei Yu, Zhu H-I, Li G-R (2021b) Influence of the roots of mixed-planting species on the shear strength

- of saline loess soil. *J Mt Sci-Engl* 18(3):1–13. <https://doi.org/10.1007/S11629-020-6169-1>
- Liu Y-F, Meng L-C, Huang Ze, Shi Z-H, Gao-Lin Wu (2022) Contribution of fine roots mechanical property of Poaceae grasses to soil erosion resistance on the Loess Plateau. *Geoderma* 426:116122. <https://doi.org/10.1016/J.GEODERMA.2022.116122>
- Lou Y, Kang H, Wang W, Guo M, Guo W, Xiao H (2022) Vertical distribution of vegetation roots and its influence on soil erosion resistance along gully headwalls in the gullied Loess Plateau. *J Soil Sediment* 23(3):1265–1280. <https://doi.org/10.1007/S11368-022-03395-6>
- Lu J, Zhang Qi, Werner AD, Li Y, Jiang S, Tan Z (2020) Root-induced changes of soil hydraulic properties – a review. *J Hydrol* 589:125203. <https://doi.org/10.1016/j.jhydrol.2020.125203>
- Luo J, Zheng Z, Li T, He S (2018) Changes in micro-relief during different water erosive stages of purple soil under simulated rainfall. *Sci Rep* 8(1):3483. <https://doi.org/10.1038/s41598-018-21852-6>
- Mao Z, Saint-André L, Genet M, Mine F-X, Jourdan C, Rey H, Courbaud B, Stokes A (2012) Engineering ecological protection against landslides in diverse mountain forests: Choosing cohesion models. *Ecol Eng* 45:55–69. <https://doi.org/10.1016/j.ecoleng.2011.03.026>
- Parhizkar M, Shabanpour M, Lucas-Borja ME, Zema DA (2021) Hydromulch roots reduce rill detachment capacity by overland flow in deforested hillslopes. *J Hydrol* 598:126272. <https://doi.org/10.1016/J.JHYDROL.2021.126272>
- Pang Y, Tian J, Yang H, Zhang K, Wang D (2022) Responses of fine roots at different soil depths to different thinning intensities in a secondary forest in the Qinling Mountains, China. *Biology* 11(3):351. <https://doi.org/10.3390/BIOLOGY11030351>
- Prats SA, Malvar MC, Coelho COA, Wagenbrenner JW (2019) Hydrologic and erosion responses to compaction and added surface cover in post-fire logged areas: Isolating splash, interrill and rill erosion. *J Hydrol* 575:408–419. <https://doi.org/10.1016/j.jhydrol.2019.05.038>
- Reubens B, Poesen J, Danjon F, Geudens G, Muys B (2007) The role of fine and coarse roots in shallow slope stability and soil erosion control with a focus on root system architecture: a review. *Trees-Struct Funct* 21(4):385–402. <https://doi.org/10.1007/s00468-007-0132-4>
- Rose L, Lobet G, Börger L (2019) Accuracy of image analysis tools for functional root traits: a comment on Delory et al. (2017). *Methods Ecol Evol* 10(5):702–711. <https://doi.org/10.1111/2041-210x.13156>
- Shahzad T, Chenu C, Genet P, Barot S, Perveen N, Mougin C, Fontaine S (2015) Contribution of exudates, arbuscular mycorrhizal fungi and litter depositions to the rhizosphere priming effect induced by grassland species. *Soil Biol Biochem* 80:146–155. <https://doi.org/10.1016/j.soilbio.2014.09.023>
- Stokes A, Atger C, Bengough AG, Fourcaud T, Sidle RC (2009) Desirable plant root traits for protecting natural and engineered slopes against landslides. *Plant Soil* 324(1–2):1–30. <https://doi.org/10.1007/s11104-009-0159-y>
- Stokes A, Douglas GB, Fourcaud T, Giadrossich F, Gillies C, Hubble T, Kim JH, Loades KW, Mao Z, McIvor IR, Mickovski SB, Mitchell S, Osman N, Phillips C, Poesen J, Polster D, Preti F, Raymond P, Rey F, Schwarz M, Walker LR (2014) Ecological mitigation of hillslope instability: ten key issues facing researchers and practitioners. *Plant Soil* 377(1/2):1–23. <https://doi.org/10.1007/s11104-014-2044-6>
- Sun S, Chen Z, Jiang H, Zhang L (2018) Black film mulching and plant density influencing soil water temperature conditions and maize root growth. *Vadose Zone J* 17(1):1–12. <https://doi.org/10.2136/vzj2018.05.0104>
- Tao H, Lei SW, Gong L, Shi X, Zhang MM, Yang GQ (2023) Study on erosion and stability of the ecological slope. *Front Earth Sci* 10:1071231. <https://doi.org/10.3389/FEART.2022.1071231>
- Tao M, Wenzhi Z, Guoqing L, Jingwei W, Jiesheng H (2021) Predicting the rooting depth, dynamic root distribution and the yield of sunflower under different soil salinity and nitrogen applications. *Ind Crop Prod* 170:113749. <https://doi.org/10.1016/J.INDCROP.2021.113749>
- Tian N, Fang S, Yang W, Shang X, Xiangxiang Fu (2017) Influence of container type and growth medium on seedling growth and root morphology of *Cyclocarya paliurus* during nursery culture. *Forests* 8(10):387. <https://doi.org/10.3390/f8100387>
- Vannoppen W, De Baets S, Keeble J, Dong Y, Poesen J (2017) How do root and soil characteristics affect the erosion-reducing potential of plant species? *Ecol Eng* 109:186–195. <https://doi.org/10.1016/j.ecoleng.2017.08.001>
- Vannoppen W, Poesen J, Peeters P, De Baets S, Vandevorode B (2016) Root properties of vegetation communities and their impact on the erosion resistance of river dikes. *Earth Surf Proc Land* 41(14):2038–2046. <https://doi.org/10.1002/esp.3970>
- Vannoppen W, Vanmaercke M, De Baets S, Poesen J (2015) A review of the mechanical effects of plant roots on concentrated flow erosion rates. *Earth-Sci Rev* 150:666–678. <https://doi.org/10.1016/j.earscirev.2015.08.011>
- Wang B, Guang-Hui Zhang XC, Zhang Z-W, Zi-Long Su, Yi T, Shi Y-Y (2014) Effects of near soil surface characteristics on soil detachment by overland flow in a natural succession grassland. *Soil Sci Soc Am J* 78(2):589–597. <https://doi.org/10.2136/sssaj2013.09.0392>
- Wang B, Li P-P, Huang C-H, Liu G-B, Yang Y-F (2020) Effects of root morphological traits on soil detachment for ten herbaceous species in the Loess Plateau. *Sci Total Environ* 754:142304. <https://doi.org/10.1016/j.scitotenv.2020.142304>
- Wang B, Zhang G-H (2017) Quantifying the binding and bonding effects of plant roots on soil detachment by overland flow in 10 typical grasslands on the Loess Plateau. *Soil Sci Soc Am J* 81(6):1567–1576. <https://doi.org/10.2136/sssaj2017.07.0249>
- Wang B, Zhang G-H, Yang Y-F, Li P-P, Liu J-X (2018) Response of soil detachment capacity to plant root and soil properties in typical grasslands on the Loess Plateau. *Age Ecosyst Environ* 266:68–75. <https://doi.org/10.1016/j.agee.2018.07.016>
- Wang J-F, Yang Y-F, Liu G-B, Wang B, Zhang F-B, Fang N-F (2023) Investigating the effects of herbaceous root systems on the soil detachment process at the species level. *Sci Total Environ* 859(P1):160196. <https://doi.org/10.1016/J.SCITOTENV.2022.160196>
- Wang J-F, Yang Y-F, Wang B, Liu G-B, Li J-M (2022a) Soil detachment caused by flowing water erosion in six typical herbaceous plant root systems on the Loess Plateau, China. *Biosyst Eng* 217:56–67. <https://doi.org/10.1016/J.BIOSYSTEMSENG.2022.03.001>
- Wang P, Mou Pu, Lingyan Hu, Shuijin Hu (2022b) Effects of nutrient heterogeneity on root foraging and plant growth at the individual and community level. *J Exp Bot* 73(22):7503–7515. <https://doi.org/10.1093/JXB/ERAC358>
- Wang Z, Zhang H, Weigang Xu, Wang H, Huang H (2019) Effects of emergent vegetation patterns on flow velocity, turbulence, and erosion around river banks. *Iran J Sci Technol Trans Civ Eng* 43(3):509–519. <https://doi.org/10.1007/s40996-018-0200-6>
- Wen X, Zhen L (2020) Soil erosion control practices in the Chinese Loess Plateau: a systematic review. *Environ Dev* 34:100493. <https://doi.org/10.1016/j.envdev.2019.100493>
- Wu G-L, Liu Yu, Fang N-F, Deng L, Shi Z-H (2016) Soil physical properties response to grassland conversion from cropland on the semi-arid area. *Ecology* 9(8):1471–1479. <https://doi.org/10.1002/eco.1740>
- Yang F, Zhong Y, Han G, Li X, Luo Li, Cai X, Long X, Li T, Huang L (2023) Effect of different vegetation restoration on soil organic carbon dynamics and fractions in the Rainy Zone of Western China. *J Environ Manage* 331:117296. <https://doi.org/10.1016/J.JENVMAN.2023.117296>
- Yang H, Zhang Q, Dai Y, Liu Q, Tang J, Bian X, Chen X (2014) Effects of arbuscular mycorrhizal fungi on plant growth depend on root

- system: a meta-analysis. *Plant Soil* 389(1–2):361–374. <https://doi.org/10.1007/s11104-014-2370-8>
- Yang Q, Zhang C, Yao S, Jiang J (2022) Root distribution and root cohesion of two herbaceous plants in the Loess Plateau of China. *Sustainability-Basel* 14(13):8053. <https://doi.org/10.3390/SU14138053>
- Ye C, Guo Z, Li Z, Cai C (2017) The effect of Bahiagrass roots on soil erosion resistance of Aquults in subtropical China. *Geomorphology* 285:82–93. <https://doi.org/10.1016/j.geomorph.2017.02.003>
- Zanchi CS, Silva AO, Batista ÉR, Peixoto DS, Barbosa MV, dos Santos JV, Alvarenga IFS, Silva BM, Carneiro MAC (2022) Pre-cultivation with herbaceous plants assists in the revegetation process of iron mining tailings with *Enterolobium contortisiliquum*. *Water Air Soil Poll* 233(7):231. <https://doi.org/10.1007/S11270-022-05696-5>
- Zhang B, Zhang G, Yang H, Zhu P (2019) Temporal variation in soil erosion resistance of steep slopes restored with different vegetation communities on the Chinese Loess Plateau. *CATENA* 182(C):104170. <https://doi.org/10.1016/j.catena.2019.104170>
- Zhang C-B, Chen L-H, Jiang J (2014) Why fine tree roots are stronger than thicker roots: the role of cellulose and lignin in relation to slope stability. *Geomorphology* 206:196–202. <https://doi.org/10.1016/j.geomorph.2013.09.024>
- Zhao C, Nie Y-H, Xin J-P, Zhu X-y, Li Y, Tian R-N (2023) Soil erosion effectively alleviated by *Miscanthus sacchariflorus*, a potential candidate for land deterioration improvement. *Rhizosphere-Neth* 26:100694. <https://doi.org/10.1016/J.RHISPH.2023.100694>
- Zhong R-H, He X-B, Bao Y-H, Tang Q, Gao J-Z, Yan D-D, Wang M-F, Li Yu (2016) Estimation of soil reinforcement by the roots of four post-dam prevailing grass species in the riparian zone of Three Gorges Reservoir, China. *J Mt Sci-Engl* 13(3):508–521. <https://doi.org/10.1007/s11629-014-3397-2>
- Zhong R-H, Jin-ming Hu, Bao Y-H, Wang F, He X-B (2018) Soil nutrients in relation to vertical roots distribution in the riparian zone of Three Gorges Reservoir, China. *J Mt Sci-Engl* 15(7):1498–1509. <https://doi.org/10.1007/s11629-017-4719-y>
- Zou H, Gao G, Yuan C, Yang W (2023) Interactions between soil water and plant community during vegetation succession in the restored grasslands on the Loess Plateau of China. *Land Degrad Dev* 34(5):1582–1592. <https://doi.org/10.1002/LDR.4555>

**Publisher's Note** Springer Nature remains neutral with regard to jurisdictional claims in published maps and institutional affiliations.

Springer Nature or its licensor (e.g. a society or other partner) holds exclusive rights to this article under a publishing agreement with the author(s) or other rightsholder(s); author self-archiving of the accepted manuscript version of this article is solely governed by the terms of such publishing agreement and applicable law.